J. Mol. Biol. (1998) **276**, 325–330

JMB

COMMUNICATION

Staphylococcal α-Hemolysin Can Form Hexamers in Phospholipid Bilayers

Daniel M. Czajkowsky, Sitong Sheng and Zhifeng Shao*

Department of Molecular Physiology and Biological Physics and Biophysics Program, University of Virginia School of Medicine Charlottesville, VA 22908, USA

*Corresponding author

Atomic force microscopy (AFM) was used to study the structure of the staphylococcal α-hemolysin (αHL) oligomer formed in supported phospholipid bilayers. In contrast to the recent X-ray crystallographic demonstration of a heptameric stoichiometry for the oligomer formed in deoxycholate (DOC) micelles, the high-resolution unprocessed AFM images unequivocally revealed a hexamer in these phospholipid bilayers. Independent support of this hexameric stoichiometry was obtained from the measurements of the lattice constant in the AFM images and from gel electrophoresis. Therefore, αHL can form two different, energetically stable oligomers, which differ in at least stoichiometry but perhaps subunit structure as well. Furthermore, stable, incomplete oligomers were observed in the AFM images, which may be of relevance to the mechanism by which αHL damages the cell.

Introduction

Staphylococcal α-hemolysin (αHL) is a 33.2 kDa, water-soluble protein that converts into a pore-forming homooligomer upon binding to the plasma membrane (Bhakdi & Tranum-Jensen, 1991). Like other cytolytic toxins (Bhakdi *et al*., 1996), oligomerization of αHL proceeds spontaneously upon contact with a suitable amphipathic substrate, inasmuch as apparently indistinguishable oligomers of αHL form in cell membranes, detergent deoxycholate (DOC) micelles, and pure phospholipid bilayers. For many years, the αHL oligomer was thought to be a hexamer based on electron microscopy (EM) and biochemical studies (for a summary, see Gouaux *et al*., 1994). However, recently X-ray crystallography (Song *et al*., 1996) clearly demonstrated that the αHL oligomer formed in DOC micelles is a heptamer, and since this demonstration the hexameric model has been largely disregarded (Bhakdi *et al*., 1996; Song *et al*., 1996). It was argued (Gouaux *et al*., 1994) that the image processing techniques used in EM could have imposed an artifactual symmetry onto the αHL oligomer, leading to an erroneous assessment of its subunit stoichiometry, and that the biochemical assays may not have had the required resolution to make an unambiguous assignment. However, the outer diameter of the αHL oligomer determined with EM, which should be a more reliable measurement (Ribi *et al*., 1988; Frank *et al*., 1995) than the determination of stoichiometry, was observed to be between 7 nm and 9 nm (Olofsson *et al*., 1988; Ward & Leonard, 1992), significantly smaller than the 10 nm diameter obtained by X-ray crystallography of the oligomer formed in DOC micelles (Song *et al*., 1996). This difference hence cannot simply be attributed to the limited accuracy of EM.

Since atomic force microscopy (AFM) has accurately resolved, under nearly physiological conditions, the structures and subunit stoichiometries of many soluble (Erie *et al*., 1994; Fritz *et al*., 1995; Mou *et al*., 1996a,b; Müller *et al*., 1997) and membrane proteins (Mou *et al*., 1995; Schabert *et al*., 1995; Müller *et al*., 1996; Walz *et al*., 1996) without using averaging techniques, we have applied this new approach to re-evaluate the structure of the αHL oligomer in a membrane. We have found that αHL can indeed form hexamers in phospholipid bilayers. Furthermore, analysis of the AFM images suggests that the structure of the subunit in the hexamer could be significantly different from that in the heptamer. We have observed stable, incomplete oligomers in these AFM images, which may

Abbreviations used: αHL, staphylococcal α-hemolysin; EM, electron microscopy; DOC, deoxycholate; AFM, atomic force microscopy; eggPC, egg phosphatidylcholine; BPS, bovine brain phosphatidylserine.

0022–2836/98/070325–06 $25.00/0/mb971535

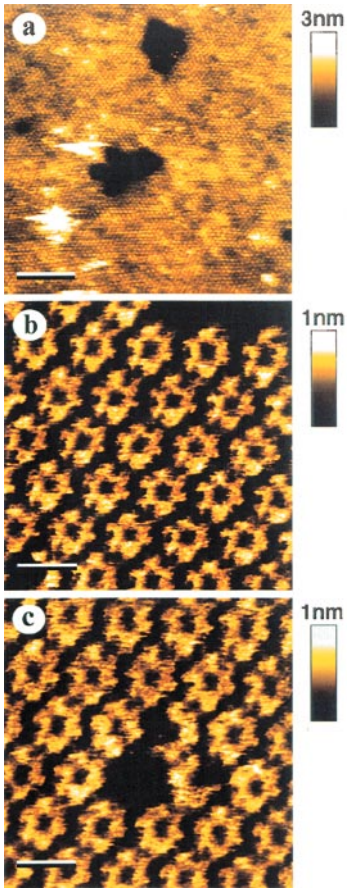

Figure 1. Unprocessed AFM images of αHL oligomers in supported bilayers in 10 mM sodium phosphate, pH 7.2 at room temperature. a, The hexagonally packed αHL oligomers can be readily detected even at this larger scan size. The dark regions are membrane defects (exposed mica); some adsorbed debris is seen (bright spots). The αHL oligomers appear well ordered (hexagonal) in only small regions, and long-range order is rather poor, which can be seen in the changes of the symmetry axes of the lattice. b, At smaller scan sizes, the structure of the individual oligomer is reproducibly resolved. Each oligomer is composed of six radial projections, 2.7(±0.3) nm ($n = 165$) in length, surrounding a central pore of 2.3(±0.3) nm ($n = 127$) in diameter, The center-to-center distance between neighboring αHL oligomers is 7.6(±0.4) nm ($n = 45$), which should be the maximal diameter of the αHL oligomer. These measurements are consistent with those observed for the hexamer in EM investigations (Olofsson *et al.*, 1988; Ward & Leonard, 1992). c, Despite the high surface concentration of complete αHL oligomers, oligomeric defects, where one or more subunits are absent, were repeatedly observed, even after hours of scanning by the tip, demonstrating that these incomplete oligomers were nonetheless energetically stable. In addition, it is clear that the general morphology of these arc-shaped complexes is similar to that of the complete hexamers, suggesting a similarity in structure at the subunit level. The slight elongation in this image is due to a piezo drift that occurs when a new region is chosen to scan. The scale bars represent: a, 100 nm; b, 7.5 nm; c, 7.5 nm.

The samples were prepared following a procedure similar to that used to grow two-dimensional crystals for EM (Uzgiris, 1986; Ribi *et al.*, 1988). The supported bilayer was formed by sequentially depositing two monolayers onto mica. The first monolayer was composed of egg phosphatidylcholine (eggPC, all lipids were obtained from Avanti Polar Lipids, Alabaster, AL) and was deposited onto a freshly cleaved fragment of mica using a Langmuir trough (J. L. Automation Ltd, England). At the same time, the second monolayer, composed of a total lipid extract from bovine heart dissolved in chloroform/methanol (2:1, v/v), was formed on the air/water interface of a small Teflon well (total volume ~40 μl). After solvent evaporation, the monolayer-covered fragment of mica was horizontally lowered onto the second monolayer to form the supported bilayer. Alpha-hemolysin (List Biochemicals, Campbell, CA), whose purity was confirmed with SDS-PAGE, was then injected into the well (through a side port), to a final concentration of about 1.5 μM in 10 mM sodium phosphate (pH 7.2). After incubation, the sample was rinsed with the same buffer and then imaged in the AFM in the same buffer used for incubation. eggPC and dioleoylphosphatidylcholine/dioleoylphosphatidylserine (1:1) have been used as the second monolayer with identical results. The buffer in most of the samples was 10 mM sodium phosphate (pH 7.2) but similar findings were observed in 10 mM Hepes (pH 7.2), 1 mM $CaCl_2$ in 1 mM sodium citrate (pH 7.2); and in 10 mM potassium phosphate (pH 7.2), 0.5 mM EGTA. Unless otherwise stated, all chemicals (reagent grade) were from Sigma Chemicals (St. Louis, MO).

All AFM images were taken in the buffer used to prepare the sample at room temperature in the contact-mode with a NonoScope II AFM (Digital Instruments, Santa Barbara, CA), retrofitted with a home-made fluid cell. Oxide-sharpened tips on Si_3N_4 cantilevers, with a nominal spring constant of 0.06 N/m, were used. Images were typically scanned at 9 Hz, and the probe force was minimized to ~0.1 nN. Two-dimensional Fourier transforms of many of the images, including those presented here, showed spots to better than 10 Å. Although no averaging was attempted, the lattice constants were determined from the two-dimensional Fourier transforms. The height was measured from cross-sectional profiles.

be relevant to the mechanism by which αHL damages a cell.

It has been established that in order to obtain high-resolution images with AFM, the molecules under study must be well adsorbed to a substrate and closely packed (Shao *et al.*, 1996). Normally, this would require high concentrations of protein incubated for long periods of time (Fang *et al.*, 1997), but these conditions were undesirable in this study because inactive oligomers of αHL can form spontaneously in solution at high concentrations (Arbuthnott *et la.*, 1967) or from proteolyzed monomers, which accumulate over time (Blomqvist *et al.*, 1987). Therefore, we developed a procedure, similar to that used in EM, using small wells in blocks of Teflon, and with this method, large supported membranes (greater than 10 μm), containing a high density of αHL oligomers, were reproducibly prepared using a relatively low concentration of toxin (less than 50 μg/ml) and with relatively short periods of incubation (less than 12 hours). As

shown in Figure 1a, the hexagonally packed αHL oligomers are clearly detected by the AFM even at somewhat larger scan sizes, and at smaller scan sizes, the size, shape and subunit stoichiometry of the oligomer are directly resolved from the unprocessed images (Figure 1b and c). The piezoscanner used in these experiments was calibrated with mica, gold ruling and the cholera toxin B-oligomer; AFM images of the latter (Mou*et al*., 1995) were consistent with both X-ray and EM measurements (Ribi *et al*., 1988; Zhang *et al*., 1995).

The AFM images show that each individual αHL oligomer in the phospholipid bilayer is unequivocally a hexamer (Figure 1b and c). This was observed reproducibly with different tips, different scan directions, and different samples under a variety of conditions, including in the presence of Ca^{2+} (1 mM $CaCl_2$), which has been shown to block the pore but not the oligomerization (Menestrina, 1986; Thelestam *et al*., 1991). The hexameric stoichiometry is further supported by the size of the lattice constant (7.6(±0.4) nm, $n = 46$) in the AFM images, which demonstrates that the maximal diameter of the oligomer is significantly smaller than that of the heptamer (10 nm) formed in DOC micelles (Song *et al*., 1996), but within the range observed with EM (Olofsson *et al*., 1988; Ward & Leonard, 1992). Since αHL oligomers, whether formed in liposomes or micelles, are stable in SDS (Bhakdi *et al*., 1981; Valeva *et al*., 1995), the sizes of the oligomers prepared under these conditions were directly compared using SDS-PAGE (Figure 2). The oligomers formed in DOC micelles migrated more slowly than the oligomers from phospholipid vesicles (eggPC to BPS, 9 : 1) with either DOC or Triton X-100 (the latter detergent does not induce oligomerization of the water-soluble monomers; Bhakdi *et al*., 1981), suggesting that the oligomers formed in DOC micelles are slightly larger. Since the oligomers formed in the bilayer and then solubilized with DOC showed the same size as those solubilized with Triton X-100, the oligomer, once formed in the bilayer, could not be converted into what forms in DOC micelles (see Figure 2, lanes B), indicating that oligomerization is not reversible and that the oligomers formed under either condition are energetically stable. So far, we have been unable to image the oligomer formed in DOC with AFM; these oligomers do not adsorb strongly to mica, which is a well-documented problem with many protein samples (Karrasch *et al*., 1993; Shao *et al*., 1996), nor do these oligomers readily incorporate into a supported membrane at a sufficiently high density (where the residual detergent is detrimental to the preformed bilayer). However, since it is reasonable to assume that the oligomers formed in DOC micelles are the same as those studied by X-ray crystallography (Song *et al*., 1996), we conclude from our observations that αHL can form oligomers with two different stoichiometries; heptamers and hexamers. Consistent with this conclusion, we note that in a recent AFM study (Fang *et al*., 1997) where images of oligomers of a mutant αHL were presented, the size of the oligomer appeared to be heterogeneous, even though a heptameric stoichiometry was concluded based on the average of 18 oligomers. At the moment, it is not known whether both oligomers can co-exist in the cell membrane, and the pathological role of two different oligomers is not clear.

Although inspection of the surface profiles suggests that the subunits in the two oligomers could be arranged similarly, a simple geometric argument, whereby one simply removes one

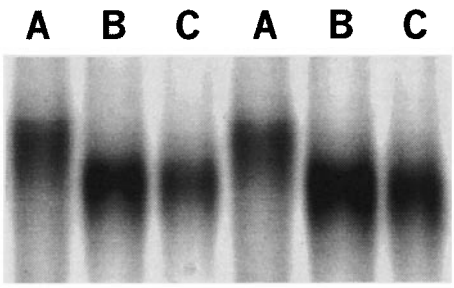

Figure 2. Comparison of the size of the αHL oligomer formed in DOC micelles with that of the oligomer formed in a membrane using 5%-SDS-PAGE. The oligomers formed in DOC micelles (lane A) migrate, as a single band, more slowly than those solubilized from phospholipid vesicles with either DOC (lanes B) or Triton X-100 (lanes C). With a shorter running time or a higher percentage acrylamide gel, a single monomer band at ~34 kDa was detected (not shown). The different migration rate indicates that the αHL oligomer formed in DOC micelles is slightly larger than that formed in the bilayer, supporting the existence of αHL oligomers of different subunit stoichiometry under these conditions. Duplicate gels are presented to indicate the reproducibility of this experiment. As a control, in the absence of lipid vesicles or DOC, only the ~34 kDa band was detected.

To prepare the membrane-induced oligomers, αHL (7.5 μM final concentration) was incubated with 10 mg/ml sonicated vesicles composed of eggPC/bovine brain phosphatidylserine (BPS; 9 : 1; the negatively charged lipid was used to prevent vesicle aggregation) for one hour in 34 mM sodium phosphate (pH 7.2). After adjusting the pH to above 8 (DOC forms large aggregates below pH 8 (Tanford & Reynolds, 1976)), either DOC (50 mM final concentration) or Triton X-100 (8 mM final concentration) was added over 30 minutes, and then incubated for an additional 30 minutes. The oligomers formed in DOC micelles were prepared by the stepwise addition of DOC (8 mM final concentration) to αHL (23 μM final concentration) in 34 mM sodium phosphate at pH 8.5 over 30 minutes, followed by an additional 30 minutes of incubation (Walker *et al*., 1992). All reactions were carried out at room temperature. All three samples were then diluted fourfold in standard non-reducing SDS-PAGE loading buffer and loaded onto the gel without heating. The gel was run for 12 hours at 4°C and then silver-stained.

subunit from the heptamer and then closes the ring, predicts that the diameter of the hexamer should be ~85% of the diameter of the heptamer, instead of the observed 76%. Whether this difference in diameter is due to different subunit structures in each oligomer remains to be determined.

The total height of the hexamer, directly measured from the surface of the mica to the top of the oligomer by AFM, is 9.7(±1.2) nm ($n = 47$), in close agreement with that depicted in the X-ray model (10 nm), although whether αHL makes direct contact with the mica could not be determined. The hexamer, however, protrudes only 5.0(±0.5) nm ($n = 76$) from the bilayer (Figure 3), compared with 7 nm estimated from the X-ray structure (Song *et al.*, 1996). This was measured whether or not the samples were fixed with glutaraldehyde, which, combined with the agreement in height between the two oligomers, indicates that there was little compression of the hexamer during imaging, as was noted previously with gap junctions (Hoh *et al.*, 1991). This suggests that the two oligomers could have substantially different structures: assuming that the subunits are structurally similar, this height would require the polar rim domain (as defined by Song *et al.*, 1996) to be completely inserted into the bilayer and the end of the hydrophobic stem to protrude farther from the bilayer than was predicted by the X-ray model (Song *et al.*, 1996).

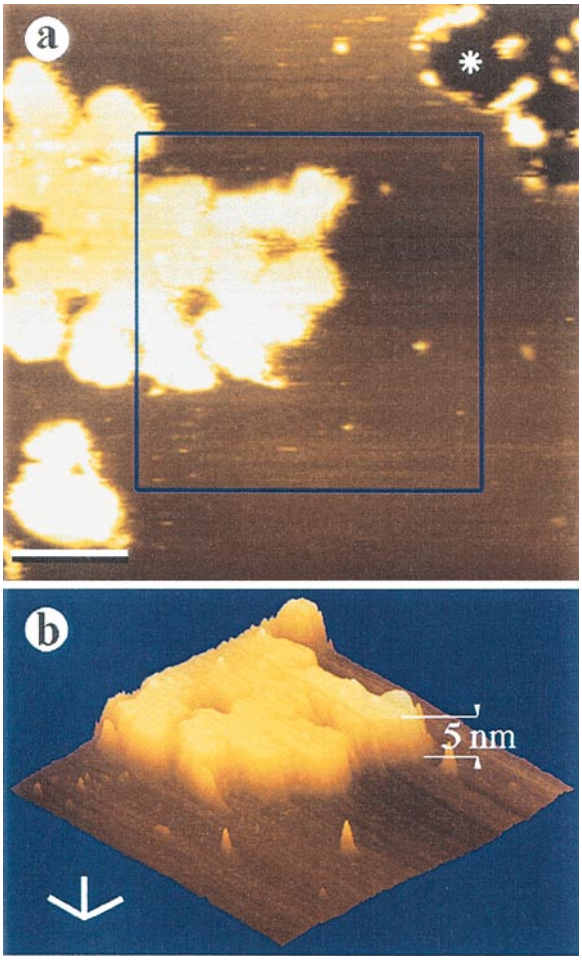

Figure 3. The height of the αHL oligomers can be determined directly from the crystal patches in an otherwise flat bilayer. a, A large-scale view to show a region of bilayer containing a large αHL oligomer patch and a membrane defect (*). The thickness of the bilayer, measured from the edge of the defect, is ~5 nm, consistent with previous AFM measurements of similar bilayers (Mou *et al.*, 1995). b, The area framed in a is presented as a surface plot to depict the amount of αHL oligomer protruding from the bilayer surface. The αHL oligomer has a height of 5 nm above the bilayer surface, which was highly reproducible with or without fixation, suggesting that vertical compression by the AFM tip, if any, was very small. This is supported by the finding that the total height of the αHL oligomer (from mica) is in good agreement with that of the X-ray structure. The scale bars represent: a, 250 nm; b, x and y 100 nm, z 6 nm.

Another intriguing observation in the AFM images is the existence of oligomeric defects, in which one or more subunits are absent from the oligomer (Figure 1c). These oligomeric defects, present despite the high surface concentration of complete oligomers, were stable even after hours of repeated scanning, indicating that these arc-shaped complexes were energetically stable in the bilayer. Moreover, the general morphology of these incomplete oligomers suggests that the structure of the subunits should be similar to that in the complete hexamer. This raises an interesting question of whether such incomplete oligomers could be a measurable fraction *in vivo*, where the toxin concentration could be much lower that the concentration used in these studies. If such incomplete oligomers remain competent in membrane insertion, there might be an additional route of membrane damage by αHL similar to that by other bacterial toxins, such as streptolysin-O and other members of the cholesterol-binding cytolysins (Alouf & Geoffroy, 1991; Tweten, 1995; Bhakdi *et al.*, 1996), which are believed to be capable of forming a pore in the membrane even when the oligomeric ring formed by these toxins is not closed.

In conclusion, staphylococcal αHL was observed to form hexamers in phospholipid bilayers, as was believed until recently. Together with the heptamers observed by X-ray crystallography, these results indicate a polymorphism of the subunit stoichiometry in the αHL oligomer. At present, the exact molecular mechanism by which αHL forms the two different oligomers is not understood, and whether the amphipathic substrate played a significant role in the formation of the two different oligomeric stoichiometries remains to be demonstrated. A full understanding of the underlying principles for the formation of one stoichiometry over the other will undoubtedly provide a valuable insight into the still poorly understood process of the assembly of membrane complexes.

Acknowledgements

We thank X. Wu for technical advice and assistance, and M. Stowell, M. Wiener, A. V. Somlyo and A. P. Somlyo for their critical reading of the manuscript. This work is supported by grants from the National Institutes of Health (RO1-RR07720 and PO1-HL48807) and the US Army Research Office (DAAL03-92-G-0002).

References

Alouf, J. E. & Geoffroy, C. (1991). The family of the antigenically related cholesterol binding cytolytic toxins. In *Sourcebook of Bacterial Toxins* (Alouf, J. E. & Freer, J. H., eds), pp. 147–186, Academic Press, London.

Arbuthnott, J. P., Freer, J. H. & Bernheimer, A. W. (1967). Physical states of staphylococcal alpha-toxin. *J. Bacteriol.* **94**, 1170–1177.

Bhakdi, S. & Tranum-Jensen, J. (1991). Alpha-toxin of *Staphylococcus aureus*. *Microbiol. Rev.* **55**, 733–751.

Bhakdi, S., Füssle, R. & Tranum-Jensen, J. (1981). Staphylococcal alpha-toxin: oligomerization of hydrophilic monomers to form amphiphilic induced through contact with deoxycholate detergent micelles. *Proc. Natl Acad. Sci. USA,* **78**, 5475–5479.

Bhakdi, S., Bayley, H., Valeva, A., Walev, I., Walker, B., Weller, U., Kehoe, M. & Palmer, M. (1996). Staphylococcal alpha-toxin, streptolysin-O, and *Escherichia coli* hemolysin: prototypes of pore forming bacterial cytolysins. *Arch. Microbiol.* **165**, 73–79.

Blomqvist, L., Bergman, T., Thelestam, M. & Jörnvall, H. (1987). Characterization of domain borders and of a naturally occurring major fragment of staphylococcal alpha-toxin. *FEBS Letters,* **211**, 127–132.

Erie, D. A., Yang, G., Schultz, H. C. & Bustamants, C. (1994). DNA bending by Cro protein in specific and nonspecific complexes: implications for protein site recognition and specificity. *Science,* **266**, 1562–1566.

Fang, Y., Cheley, S., Bayley, H. & Yang, J. (1997). The heptameric prepore of a staphylococcal alpha-hemolysin mutant lipid bilayers imaged by atomic force microscopy. *Biochemistry,* **36**, 9518–3522.

Frank, J., Zhu, J., Penczek, P., Li, Y., Srivastava, S., Verschoor, A., Radermacher, M., Grussucci, R., Lata, R. K. & Agrawal, R. K. (1995). A model of protein synthesis based on cryo-electron microscopy of the *E. coli* ribosome. *Nature,* **376**, 441–444.

Fritz, M., Radmacher, M., Cleveland, J. P., Allersma, M. W., Stewart, R. J., Gieselmann, R., Janmey, P., Schmidt, C. F. & Hansma, P. K. (1995). Imaging globular and filamentous proteins in physiological buffer solution with tapping mode atomic force microscopy. *Langmuir,* **11**, 3529–3535.

Gouaux, J. E., Braha, O., Hobaugh, M. R., Song, L., Cheley, S., Shustak, C. & Bayley, H. (1994). Subunit stoichiometry of staphylococcal alpha-hemolysin in crystals and on membranes: a heptameric transmembrane pore. *Proc. Natl Acad. Sci. USA,* **91**, 12828–12831.

Hoh, J. H., Lal, R., John, S. A., Revel, J.-P. & Arnsdorf, M. F. (1991). Atomic force microscopy and dissection of gap junctions. *Science,* **253**, 1405–1408.

Karrasch, S., Dolder, M., Schabert, F., Ramsden, J. & Engel, A. (1993). Covalent binding of biological samples to solid supports for scanning probe microscopy in buffer solution. *Biophys. J.* **65**, 2437–2446.

Menestrina, G. (1986). Ionic channels formed by *Staphylococcus aureus* alpha-toxin: voltage-dependent inhibition by divalent and trivalent cations. *J. Membr. Biol.* **90**, 17–190.

Mou, J., Yang, J. & Shao, Z. (1995). Atomic force microscopy of cholera toxin B-oligomers bound to bilayers of biologically relevant lipids. *J. Mol. Biol.* **248**, 507–512.

Mou, J., Czajkowsky, D. M., Zhang, Y. & Shao, Z. (1996a). High-resolution atomic-force microscopy of DNA: the pitch of the double helix. *FEBS Letters,* **371**, 279–282.

Mou, J., Sheng, S., Ho, R. & Shao, Z. (1996b). Chaperonins GroEL and GroES: views from atomic force microscopy. *Biophys. J.* **71**, 2213–2221.

Müller, D. J., Baumeister, W. & Engel, A. (1996). Conformational change of the hexagonally packed intermediate layer imaged by atomic force microscopy. *J. Bacteriol.* **178**, 3025–3030.

Müller, D. J., Engel, A., Carrascosa, J. L. & Vélez, M. (1997). The bacteriophage phi-29 head-tail connector imaged at high resolution with the atomic force microscope buffer solution. *EMBO J.* **16**, 2547–2553.

Olofsson, A., Kavéus, O., Thelestam, M. & Herbert, H. (100). The projection structure of alpha-toxin *Staphylococcus aureus* in human platelet membranes as analyzed by electron microscopy and imaging processing. *J. Ultrastruct. Mol. Struct. Res.* 194–200.

Ribi, H. O., Ludwig, D. S., Mercer, K. L., Schoolnik, G. K. & Kornberg, R. D. (1988). Three-dimensional structure of cholera toxin penetrating a lipid membrane. *Science,* **239**, 1272–1276.

Schabert, F. A., Henn, C. & Engel, A. (1994). Native *Escherichia coli* OmpF surfaces probed by atomic force microscopy. *Science,* **268**, 92–94.

Shao, Z., Mou, J., Czajkowsky, D. M., Yang, J. & Yuan, J.-Y. (1996). Biological atomic force microscopy: what is achieved and what is needed. *Advan. Phys.* **45**, 1–86.

Song, L., Hobaugh, M. R., Shustak, C., Cheley, S., Bayley, H. & Gouaux, J. E. (1996). Structure of staphylococcal alpha-hemolysin, a heptameric transmembrane pore. *Science,* **274**, 1859–1866.

Tanford, C. & Reynolds, J. A. (1976). Characterization of membrane protein in detergent solutions. *Biochim. Biophys. Acta,* **457**, 133–170.

Thelestam, M., Olofsson, A., Blomqvist, L. & Hebert, H. (1991). Oligomerisation of cell-bound staphylococcal alpha-toxin in relation to membrane permeabilisation. *Biochim. Biophys. Acta,* **1062**, 245–254.

Tweten, R. K. (1995). Pore forming toxins in gram positive bacteria. In *Virulence Mechanisms of Bacterial Pathogens* (Roth, J. A., Bolin, C. A., Brogden, K. A., Minion, C. & Wannemuehler, eds), pp. 207–229, Am. Soc. Microbiol., Washington, DC.

Uzgiris, E. E. (1986). Supported phospholipid bilayers for two-dimensional protein crystallization. *Biochem. Biophys. Res. Commun.* **134**, 819–826.

Valeva, A., Palmer, M., Hilgert, K., Kehoe, M. & Bhakdi, S. (1995). Correct oligomerization is a prerequisite for insertion of the central molecular domain of staphylococcal alpha-toxin into the lipid layer. *Biochim. Biophys. Acta,* **1236**, 213–218.

Walker, B., Krishnasastry, M., Zorn, L. & Bayley, H. (1992). Assembly of the oligomeric membrane pore formed by staphylococcal alpha-hemolysin examined by truncation mutagenesis. *J. Biol. Chem.* **267**, 21782–21786.

Walz, T., Tittmann, P., Fuchs, K. H., Müller, D. J., Smith, B. L., Agre, P., Gross, H. & Engel, A. (1996). Surface topographies at subnanometer resolution reveal asymmetry and sidedness of aquaporin-1. *J. Mol. Biol.* **264**, 907–918.

Ward, R. J. & Leonard, K. (1992). The *Staphylococcus aureus* alpha-toxin channel complex and the effect of Ca^{+2} ions on its interaction with lipid layers. *J. Struct. Biol.* **109**, 129–141.

Zhang, R., Westbrook, M. L., Westbrook, E. M., Scott, D. L., Otwinowski, Z., Maulik, P. R., Reed, R. A. & Shipley, G. G. (1995). The 2.4 Å crystal structure of cholera toxin B subunit pentamer: choleragenoid. *J. Mol. Biol.* **251**, 550–562.

Edited by W. Baumeister

(Received 29 September 1997; received in revised form 14 November 1997; accepted 16 November 1997)